Korean Journal of Chemical Engineering (2024) 41:869–877
https://doi.org/10.1007/s11814-024-00116-2

ORIGINAL ARTICLE

Rietveld Analysis of Binary (2,5-Dihydrofuran + Methane) and (2,3-Dihydrofuran + Methane) Clathrate Hydrates

Dong Hyun Kim[1] · Ki Hun Park[1] · Minjun Cha[1,2]

Received: 22 August 2023 / Revised: 16 September 2023 / Accepted: 18 September 2023 / Published online: 16 February 2024

Abstract

Herein, we examined the crystal structure of 2,5-dihydrofuran and 2,3-dihydrofuran clathrate hydrate systems in the presence of methane as help gas. The crystal structure of these systems demonstrates the structure II (sII) clathrate hydrate with the cubic *Fd-3m* space group. Throughout the inclusion of methane, we observed a decrease in lattice parameters for both 2,5-dihydrofuran and 2,3-dihydrofuran clathrate hydrates. In the (2,5-dihydrofuran + H_2O) or (2,3-dihydrofuran + H_2O) clathrate hydrates, the 2,5-dihydrofuran or 2,3-dihydrofuran molecule is located at the center of the large cages of sII hydrate. However, in the (2,5-dihydrofuran + CH_4) or (2,3-dihydrofuran + CH_4) binary clathrate hydrates, the 2,5-dihydrofuran or 2,3-dihydrofuran molecule is positioned off-center in the large cages of sII hydrate. Finally, we confirmed the possibility increase of host–guest interaction via possible host–guest hydrogen bonding due to the decrease of the shortest distance between host and guest molecules.

Keywords Clathrate hydrate · Rietveld analysis · Structure identification · Methane inclusion · Hydrogen bonding

Introduction

As the global demand for energy continues to rise, finding efficient and environmentally friendly methods for energy storage and transportation becomes increasingly crucial. Solidified natural gas (SNG) storage using clathrate hydrates has emerged as a promising solution, offering a novel approach to store and transport natural gas in a condensed form [1–5]. Clathrate hydrates are unique crystalline structures formed when water molecules encapsulate guest molecules, typically gases, within their cage-like framework [6, 7]. These structures resemble ice and exhibit remarkable properties, including high gas storage capacity, low density, and enhanced stability under appropriate temperature and pressure conditions [6, 7]. The gas molecules trapped within clathrate hydrates are efficiently sequestered, resulting in a denser and more manageable storage medium for natural gas [8–25].

The exploration of clathrate hydrates for gas storage dates back several decades, primarily focusing on methane hydrates because of their abundance in nature and potential as an unconventional energy resource [6, 7]. However, recent research has broadened the scope by including other guest molecules like tetrahydrofuran (THF) and cyclopentane (CP), which possess unique properties and hold promise for SNG storage applications [24, 25]. THF and CP are commonly used as thermodynamic hydrate promoters and have been proven to improve the thermodynamic conditions for methane hydrates [22–24]. Additionally, they can lower the energy required for hydrate nucleation, resulting in more efficient and faster hydrate formation. These characteristics make THF and CP effective additives for enhancing the storage and transportation of methane using gas hydrates. 2,5-dihydrofuran and 2,3-dihydrofuran are heterocyclic compounds that share similarities with THF and CP, possessing comparable size, shape, and molecular weight [26]. Furthermore, similar to THF and CP, 2,5-dihydrofuran and 2,3-dihydrofuran are known to be capable of self-forming structure II hydrates [6, 7, 27, 28]. In this

Dong Hyun Kim and Ki Hun Park contributed equally to this work.

✉ Minjun Cha
minjun.cha@kangwon.ac.kr

[1] Department of Integrated Energy and Infra System, Kangwon National University, 1 Kangwondaehak-gil, Chuncheon-si 24341, Gangwon-do, Republic of Korea

[2] Department of Energy and Resources Engineering, Kangwon National University, 1 Kangwondaehak-gil, Chuncheon-si 24341, Gangwon-do, Republic of Korea

perspective, 2,5-dihydrofuran and 2,3-dihydrofuran can be considered as potential candidates, similar to THF and CP, for utilization in SNG applications. However, considering the lack of structural analysis studies on clathrate hydrates of 2,5-dihydrofuran and 2,3-dihydrofuran containing methane, this research aims to address this gap by conducting a comprehensive investigation.

This study aims to investigate the crystal structure of binary (2,5-dihydrofuran + methane) and (2,3-dihydrofuran + methane) clathrate hydrates. The characteristic behaviors of the 2,5-dihydrofuran and 2,3-dihydrofuran guest molecules in the hydrate cages were investigated via structural identification using high-resolution powder X-ray diffraction (HRPD) with Rietveld refinement.

Experimental Details

Distilled H_2O (Samchun Pure Chemical, Pyeongtaek-si, South Korea), 2,5-dihydrofuran (98.0 mol% purity, Tokyo Chemical Industry), 2,3-dihydrofuran (98.0 mol% purity, Tokyo Chemical Industry), and CH_4 gas (99.95 mol% purity, Korea Nano Gas) were used for synthesizing the binary (2,5-dihydrofuran + methane) and (2,3-dihydrofuran + methane) clathrate hydrates.

To prepare the binary (2,5-dihydrofuran + methane) and (2,3-dihydrofuran + methane) clathrate hydrates samples, a 5.56 mol% 2,5-dihydrofuran or 2,3-dihydrofuran solution was placed in a freezer (~ 193 K) under atmospheric pressure for one hour. And then, the frozen sample was ground to 100 μm under liquid nitrogen condition. Here, we used half of the resulting fine powder as (2,5-dihydrofuran + H_2O) and (2,3-dihydrofuran + H_2O) hydrate (without methane help gas) samples. And then, remaining half of the resulting fine powder was put into the pressure vessel, and then the reactor vessel was pressurized with CH_4 up to 8.0 MPa. The reactor vessel was kept in a bath circulator (~ 269 K) for a week for the formation of the binary (2,5-dihydrofuran + methane) and (2,3-dihydrofuran + methane) clathrate hydrates samples. The formed hydrate samples were recovered under liquid nitrogen condition, and then ground again.

For the structure identifications of as (2,5-dihydrofuran + H_2O) and (2,3-dihydrofuran + H_2O) hydrate, and of the binary (2,5-dihydrofuran + methane) and (2,3-dihydrofuran + methane) hydrates, high-resolution powder X-ray diffraction (HRPD) patterns of our hydrate samples were acquired at 100 K using the 2D Supramolecular Crystallography beamline (with a synchrotron radiation of 0.90000 Å) at the Pohang Accelerator Laboratory (PAL) [29]. The detailed experimental procedures can be seen in our previous studies [30–33]. The obtained HRPD patterns were refined using the FullProf program and the FOX program for the Rietveld analyses with Direct Space method [34–37].

Results & Discussion

The crystal structure and guest inclusion behaviors of the binary (2,5-dihydrofuran + methane) and (2,3-dihydrofuran + methane) clathrate hydrates were investigated via structural identification using high-resolution powder X-ray diffraction (HRPD) with Rietveld refinement (with Direct Space method) [34, 35]. The structural refinement of our HRPD patterns was performed using the FullProf program and the FOX program [36, 37]. The structural model of guest molecules (2,5-dihydrofuran, 2,3-dihydrofuran, and methane) was geometrically optimized using the CASTEP module with the GGA-BLYP model in the Materials Studio program (Fig. 1) [38]. 2,5-dihydrofuran and 2,3-dihydrofuran are similar to THF and CP, respectively, with comparable sizes, shapes, and molecular weights. In addition, 2,5-dihydrofuran and 2,3-dihydrofuran are known to be a structure II (sII) hydrate-forming agent without the help gas [6, 7, 27, 28]. Therefore, we also identified the crystal structure of (2,5-dihydrofuran + H_2O) and (2,3-dihydrofuran + H_2O) hydrates.

In our study, the virtual atomic species, such as CH_4, $–CH_2–$, –CH–, and H_2O, were used by using the sum of individual atomic scattering factors. Followings are the refined variables: zero shift, scale, peak shape, and thermal displacement parameters, atomic coordinates, lattice parameters, and site occupancies. The 2,5-dihydrofuran

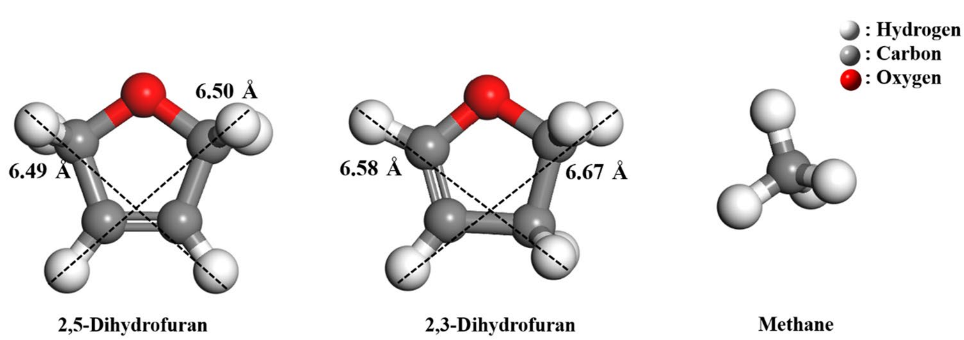

Fig. 1 The optimized molecular structure of 2,5-dihydrofuran, 2,3-dihydrofuran, and methane and their molecular size (Gray, carbon; white, hydrogen; red, oxygen)

or 2,3-dihydrofuran molecule in the hydrate cages was regarded as the rigid body and positioned at the center of the large $5^{12}6^4$ cages of sII hydrate. And then, the position of 2,5-dihydrofuran or 2,3-dihydrofuran molecule in the large $5^{12}6^4$ cages of sII hydrate was estimated via the Direct Space method [35]. CH_4 molecule can be captured in the small 5^{12} and large $5^{12}6^4$ cages of sII hydrate for the binary (2,5-dihydrofuran + methane) and (2,3-dihydrofuran + methane) clathrate hydrates, and thus, the ratio of the CH_4 molecules in the small 5^{12} and large $5^{12}6^4$ cages of sII hydrate was assumed to be 10.98 and 8.13 for the binary (2,5-dihydrofuran + methane) and (2,3-dihydrofuran + methane) clathrate hydrates from the area ratio ($A_{sII\text{-}S}/A_{sII\text{-}L}$) from the ^{13}C solid-state nuclear magnetic resonance (NMR) results (Figure S1).

In Fig. 2, the refined HRPD patterns of (2,5-dihydrofuran + H_2O) hydrate (Fig. 2a) and (2,5-dihydrofuran + methane) hydrate (Fig. 2b) are shown and the refined patterns are good with reliability factors (background corrected R_{wp} = 10.5% and $\chi^2 = 13.3$ for Fig. 2a and R_{wp} = 13.4% and $\chi^2 = 37.6$ for Fig. 2b). In Tables 1 and 2, the atomic

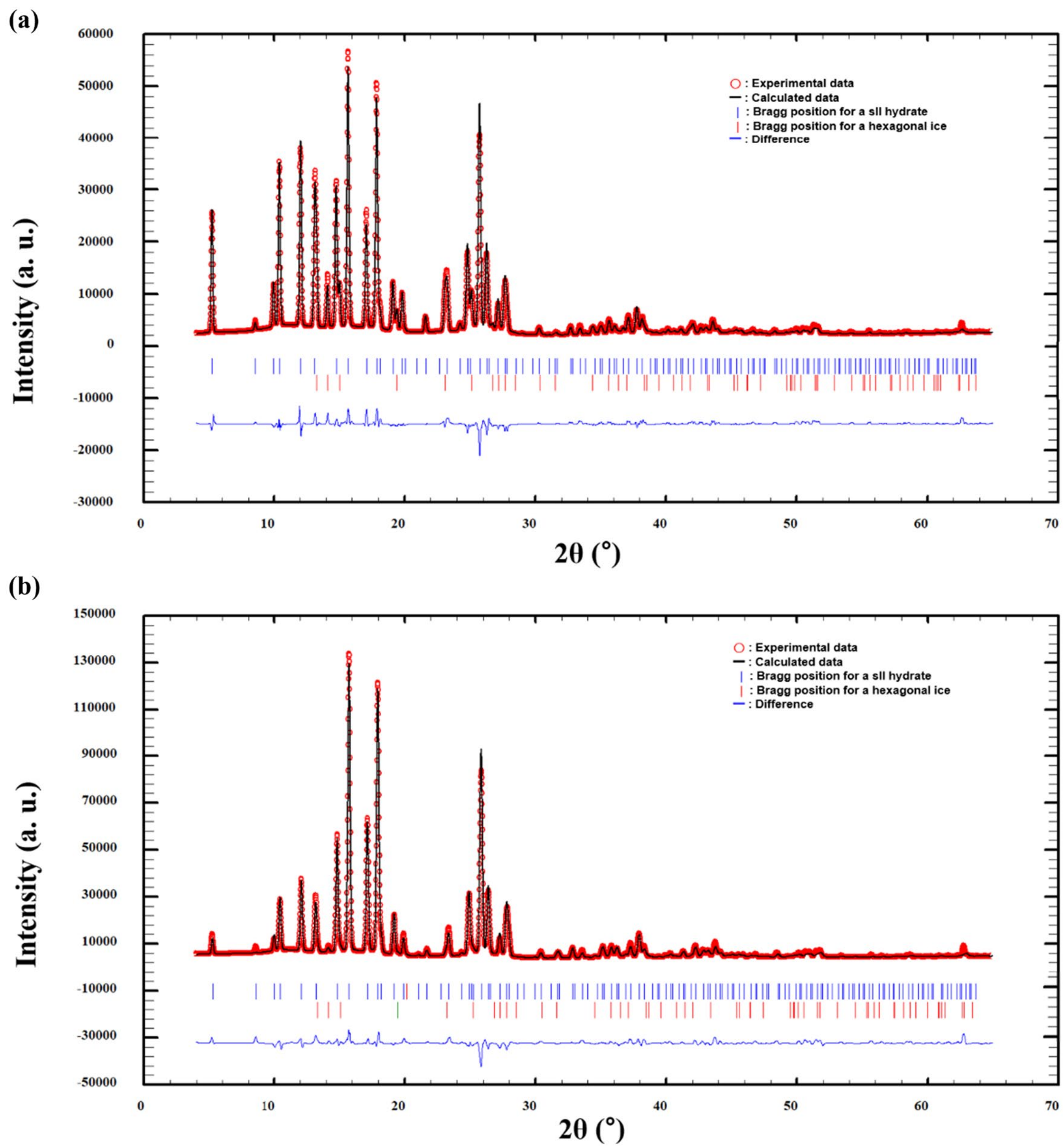

Fig. 2 Supramolecular crystallography patterns of **a** (2,5-dihydrofuran + H_2O) hydrate measured at 100 K and the Rietveld refinement results (background corrected R_{wp} = 10.5% and $\chi^2 = 13.3$), and **b** (2,5-dihydrofuran + methane) hydrate measured at 100 K and the Rietveld refinement results (background corrected R_{wp} = 13.4% and $\chi^2 = 37.6$), Tick marks indicate the Bragg position for sII hydrate and the hexagonal ice phases

Table 1 Atomic coordinates, isotropic temperature factors, and site occupancies for (2,5-Dihydrofuran + H_2O) hydrate (Wa, virtual atomic species for the host framework; LG, virtual atomic species for 2,5-Dihydrofuran)

Atom	x	y	z	B($Å^2$)	Site occupancy	Multiplicity (with Wyckoff letter)
Wa^1	0.12500	0.12500	0.12500	2.266(96)	8	8 a
Wa^2	0.21706(5)	0.21706	0.21706	3.161(67)	32	32 e
Wa^3	0.18188(3)	0.18188	0.37061(5)	3.549(37)	96	96 *g*
LG^1 (CH_2 in 2,5-Dihydrofuran)	0.32694	0.34865	0.43987	12.720	7.96834	192 ***i***
LG^2 (CH in 2,5-Dihydrofuran)	0.34587	0.43343	0.42775	12.720	7.96834	192 ***i***
LG^3 (CH in 2,5-Dihydrofuran)	0.40263	0.44060	0.37542	12.720	7.96834	192 ***i***
LG^4 (CH_2 in 2,5-Dihydrofuran)	0.42744	0.36134	0.34722	12.720	7.96834	192 ***i***
LG^5 (O in 2,5-Dihydrofuran)	0.37888	0.30737	0.38886	12.720	7.96834	192 ***i***

Table 2 Atomic coordinates, isotropic temperature factors, and site occupancies for (2,5-Dihydrofuran + CH_4) hydrate (Wa, virtual atomic species for the host framework; SG, virtual atomic species for methane; LG, virtual atomic species for 2,5-Dihydrofuran)

Atom	x	y	z	B($Å^2$)	Site occupancy	Multiplicity (with Wyckoff letter)
Wa^1	0.12500	0.12500	0.12500	2.121(103)	8	8 a
Wa^2	0.21740(7)	0.21740	0.21740	3.172(78)	32	32 e
Wa^3	0.18247(4)	0.18247	0.37163(7)	3.207(41)	96	96 *g*
SG^S (CH_4 in the small cages of sII hydrate)	0.49875	0.24967	0.74923	1.608	9.738	192 ***i***
SG^L (CH_4 in the large cages of sII hydrate)	0.37500	0.37500	0.37500	15.183	0.886	8 *b*
LG^1 (CH_2 in 2,5-Dihydrofuran)	0.37415	0.36468	0.43560	15.183	7.109	192 ***i***
LG^2 (CH in 2,5-Dihydrofuran)	0.41285	0.44336	0.42728	15.183	7.109	192 ***i***
LG^3 (CH in 2,5-Dihydrofuran)	0.44457	0.44995	0.35648	15.183	7.109	192 ***i***
LG^4 (CH_2 in 2,5-Dihydrofuran)	0.43030	0.37636	0.31025	15.183	7.109	192 ***i***
LG^5 (O in 2,5-Dihydrofuran)	0.38683	0.32632	0.36190	15.183	7.109	192 ***i***

coordinates, thermal displace parameters, and site occupancies of the refined (2,5-dihydrofuran + H_2O) hydrate (Fig. 2a) and (2,5-dihydrofuran + methane) hydrate (Fig. 2b) are listed. The refined results showed that the crystal structure of (2,5-dihydrofuran + H_2O) hydrate (Fig. 2a) and (2,5-dihydrofuran + methane) hydrate (Fig. 2b) was identified as the cubic *Fd-3m* space group with lattice parameters of 17.13486(36) and 17.06365(59) Å. In addition, the hexagonal $P6_3/mmc$ structure of the hexagonal ice could be also observed in the refined PXRD patterns (Fig. 2). The calculated weight fraction of (2,5-dihydrofuran + H_2O) hydrate was approximately 87.34%, with the impurity hexagonal ice (*Ih*) for the remaining 12.66%. And the calculated weight fraction of the binary (2,5-dihydrofuran + methane) hydrate was 98.34%, with the impurity hexagonal ice (*Ih*) for the remaining 1.66%. Similarly, Fig. 3 shows the refined HRPD patterns (with reliability factors, background corrected R_{wp} = 11.0% and $\chi^2 = 19.5$ for Fig. 3a and R_{wp} = 13.5% and $\chi^2 = 33.7$ for Fig. 3b) of (2,3-dihydrofuran + H_2O) hydrate and (2,3-dihydrofuran + methane) hydrate (Tables 3 and 4). The lattice parameters for (2,3-dihydrofuran + H_2O) hydrate and (2,3-dihydrofuran + methane) hydrate were reported as 17.12526(51) and 17.04578(66) Å. The calculated weight fraction of (2,3-dihydrofuran + H_2O) hydrate was approximately 63.16%, with the impurity hexagonal ice (*Ih*) for the remaining 36.84%. Similarly, the calculated weight fraction of the binary (2,3-dihydrofuran + methane) hydrate was 66.13%, with the impurity hexagonal ice (*Ih*), and structure I hydrate accounting for the remaining 31.87%, and 2.01%, respectively. One notable thing is the decrease of lattice parameters during the methane encapsulation in the hydrate cages for both 2,5-dihydrofuran and 2,3-dihydrofuran clathrate hydrates. Kawamura et al. [39] reported that the lattice parameters of THF and 2,5-dihydrofuran clathrate hydrates decreased during the enclathration of hydrogen molecules in the empty 5^{12} cages of sII hydrate. Similarly, the decrease of lattice parameters in our hydrate systems during the enclathration of methane molecules in the hydrate cages can be observed, and these phenomena may be related to the intermolecule interaction between methane guest molecule and host water or 2,5-dihydrofuran (or 2,3-dihydrofuran) [39]. To clearly understand the host–guest and guest–guest

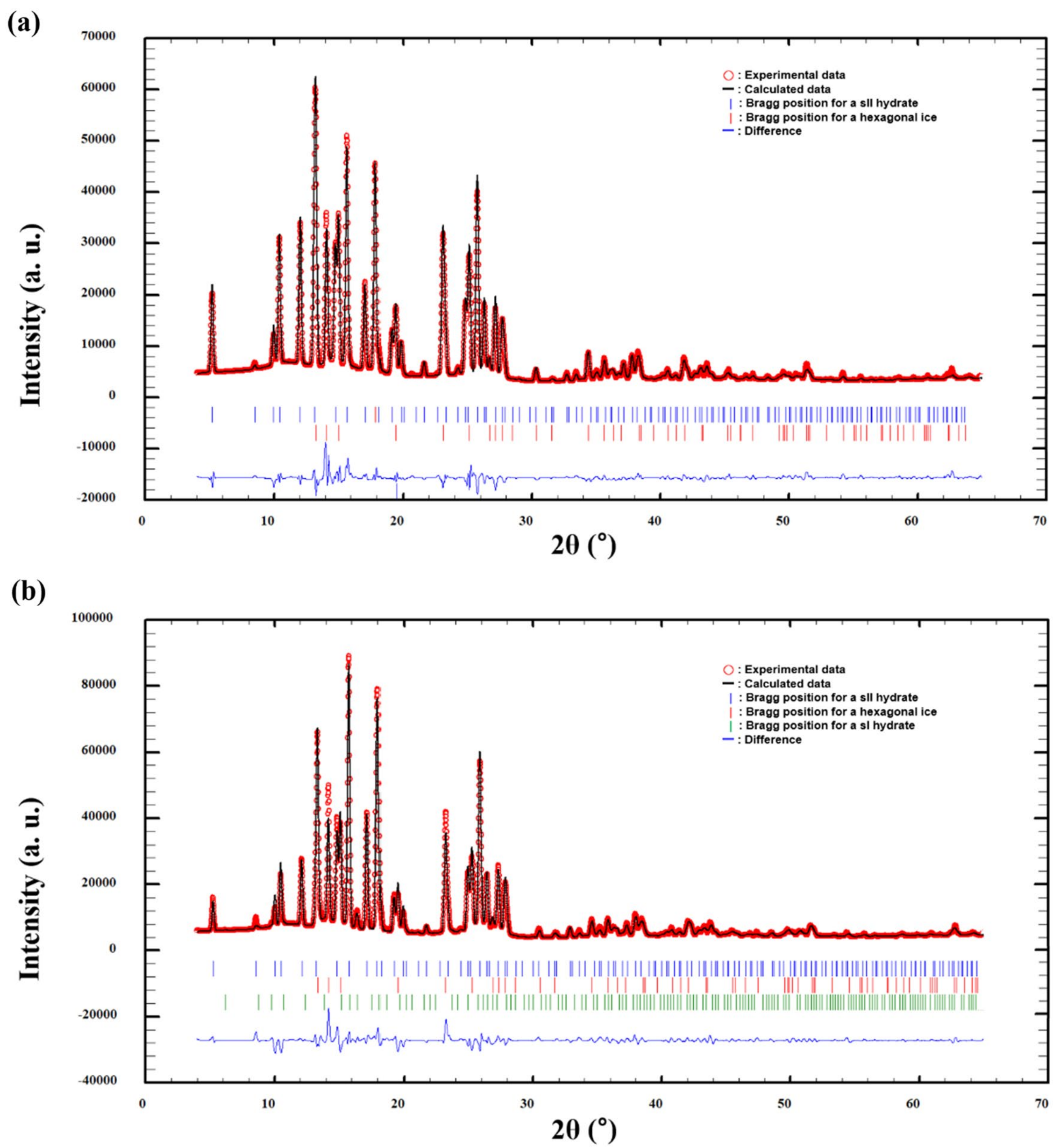

Fig. 3 Supramolecular crystallography patterns of **a** (2,3-dihydrofuran + H_2O) hydrate measured at 100 K and the Rietveld refinement results (background corrected R_{wp} = 11.0% and χ^2 = 19.5), and **b** (2,3-dihydrofuran + methane) hydrate measured at 100 K and the Rietveld refinement results (background corrected R_{wp} = 13.5% and χ^2 = 33.7), Tick marks indicate the Bragg position for sII hydrate, the hexagonal ice, and sI hydrate phases

interactions by adding the methane molecule in the hydrate system, further studies using ab initio modeling should be performed in the future.

In Figs. 4 and 5, 2,5-dihydrofuran, 2,3-dihydrofuran, and methane molecules with full symmetries in the large $5^{12}6^4$ (for 2,5-dihydrofuran and 2,3-dihydrofuran) and small 5^{12} (for methane molecules) cages of sII hydrates are given. During the Rietveld analysis of our HRPD patterns, the position of 2,5-dihydrofuran or 2,3-dihydrofuran molecule in the large $5^{12}6^4$ cages of sII hydrate was estimated via the Direct Space method (using FOX program) [35, 37]. And then, the results showed that the 2,5-dihydrofuran or 2,3-dihydrofuran molecule in the case of (2,5-dihydrofuran + H_2O) or (2,3-dihydrofuran + H_2O) clathrate hydrates is almost positioned at the center of large $5^{12}6^4$ cages of sII hydrate (Figs. 4a and 5a), but the 2,5-dihydrofuran or 2,3-dihydrofuran molecule in the case of the binary (2,5-dihydrofuran + CH_4) and (2,3-dihydrofuran + CH_4) clathrate

Table 3 Atomic coordinates, isotropic temperature factors, and site occupancies for (2,3-Dihydrofuran + H_2O) hydrate (Wa, virtual atomic species for the host framework; SG, virtual atomic species for methane; LG, virtual atomic species for 2,3-Dihydrofuran)

Atom	x	y	z	B(Å^2)	Site occupancy	Multiplicity (with Wyckoff letter)
Wa^1	0.12500	0.12500	0.12500	2.324(144)	8	8 a
Wa^2	0.21724(8)	0.21724	0.21724	2.687(89)	32	32 e
Wa^3	0.18196(4)	0.18196	0.37056(8)	2.700(47)	96	96 *g*
LG^1 (CH_2 in 2,3-Dihydrofuran)	0.17353	0.07504	0.59539	12.265(398)	7.831(28)	192 ***i***
LG^2 (CH_2 in 2,3-Dihydrofuran)	0.14367	0.15241	0.55898	12.265	7.831	192 ***i***
LG^3 (CH in 2,3-Dihydrofuran)	0.11507	0.19582	0.63048	12.265	7.831	192 ***i***
LG^4 (CH in 2,3-Dihydrofuran)	0.12673	0.15144	0.69319	12.265	7.831	192 ***i***
LG^5 (O in 2,5-Dihydrofuran)	0.16021	0.08039	0.67929	12.265	7.831	192 ***i***

Table 4 Atomic coordinates, isotropic temperature factors, and site occupancies for (2,3-Dihydrofuran + H_2O) hydrate (Wa, virtual atomic species for the host framework; SG, virtual atomic species for methane; LG, virtual atomic species for 2,3-Dihydrofuran)

Atom	x	y	z	B(Å^2)	Site occupancy	Multiplicity (with Wyckoff letter)
Wa^1	0.12500	0.12500	0.12500	4.306(199)	8	8 a
Wa^2	0.22102	0.22102	0.22102	6.930(144)	32	32 e
Wa^3	0.18191	0.18191	0.37387	3.963(59)	96	96 *g*
SG^S (CH_4 in the small cages of sII hydrate)	0.01205	0.25037	0.26162	0.001	7.715	192 ***i***
SG^L (CH_4 in the large cages of sII hydrate)	0.37500	0.37500	0.37500	13.655	1.124	8 *b*
LG^1 (CH_2 in 2,3-Dihydrofuran)	0.29686	0.86157	0.85095	13.655	6.871	192 ***i***
LG^2 (CH_2 in 2,3-Dihydrofuran)	0.33159	0.82933	0.77328	13.655	6.871	192 ***i***
LG^3 (CH in 2,3-Dihydrofuran)	0.40793	0.79364	0.80131	13.655	6.871	192 ***i***
LG^4 (CH in 2,3-Dihydrofuran)	0.41395	0.80418	0.87843	13.655	6.871	192 ***i***
LG^5 (O in 2,5-Dihydrofuran)	0.35280	0.84288	0.91288	13.655	6.871	192 ***i***

hydrates is off-centered at the center of large $5^{12}6^4$ cages of sII hydrate (Figs. 4b and 5b). Therefore, the distances between host and guest molecules in the large $5^{12}6^4$ cages of sII hydrate for the binary (2,5-dihydrofuran + CH_4) and (2,3-dihydrofuran + CH_4) clathrate hydrates also changed (Figs. 6 and 7). Figure 6 shows that the shortest distances between host water and guest 2,5-dihydrofuran molecules decrease from 3.32 to 2.91 Å during the enclathration of methane molecule in the hydrate cages [40]. Similar trends are observed in Fig. 7 for 2,3-dihydrofuran hydrate systems (3.36 to 2.78 Å) during the enclathration of methane molecule. With the decrease of the shortest distances between host water and guest molecules in the large $5^{12}6^4$ cages of sII hydrate, we may clearly conclude that there is the increase of guest–host interaction via possible hydrogen bonding interactions during the methane inclusion behaviors. Again, the enclathration of methane molecules in the hydrate cages may affect the inter-molecule interaction between host–guest and guest–guest molecules, and the unanswered nature of host-guest inclusion chemistry should be clearly understood in the future.

In present studies, we identified the crystal structure of 2,5-dihydrofuran and 2,3-dihydrofuran clathrate hydrate systems with/without methane help gas. The characteristic behaviors of the 2,5-dihydrofuran and 2,3-dihydrofuran guest molecules with/without methane help gas in the hydrate cages were demonstrated via Rietveld analysis with the Direct Space method. The results of this study may provide the useful information on the unique nature of host–guest inclusion compounds.

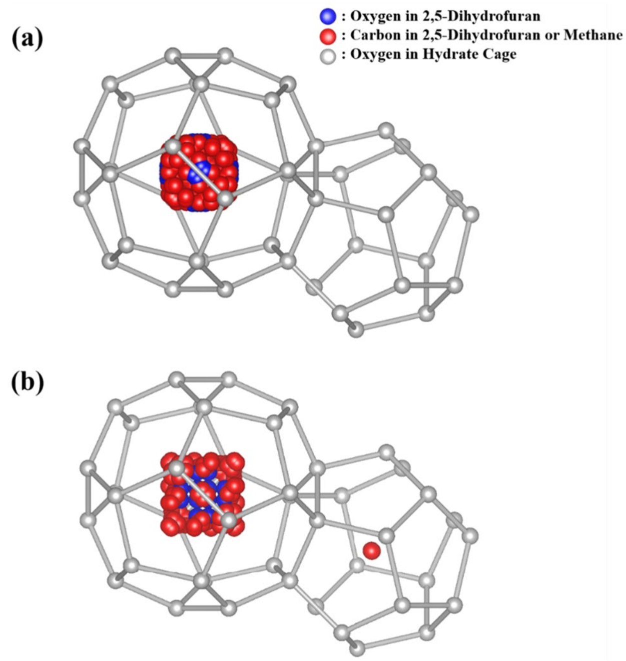

Fig. 4 Crystal structure and guest positions of **a** (2,5-dihydrofuran + H_2O) hydrate, and **b** (2,5-dihydrofuran + methane) hydrate obtained by Rietveld analysis. Distribution of guest molecules in small and large cages of (2,5-dihydrofuran + H_2O) hydrate, and (2,5-dihydrofuran + methane) hydrate with full symmetry

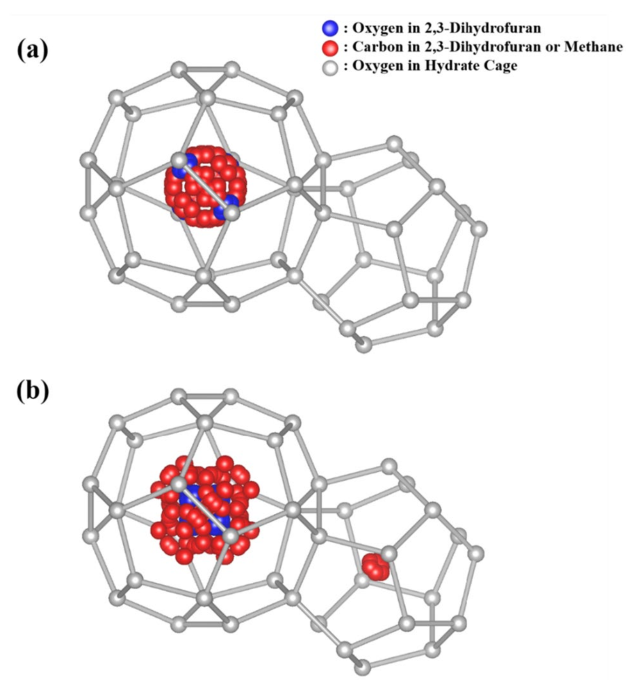

Fig. 5 Crystal structure and guest positions of **a** (2,3-dihydrofuran + H_2O) hydrate, and **b** (2,3-dihydrofuran + methane) hydrate obtained by Rietveld analysis. Distribution of guest molecules in small and large cages of (2,3-dihydrofuran + H_2O) hydrate, and (2,3-dihydrofuran + methane) hydrate with full symmetry

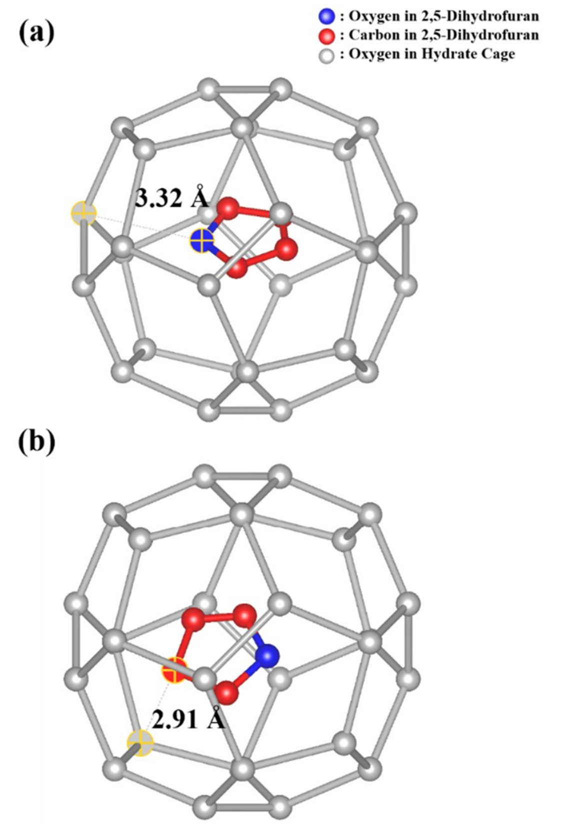

Fig. 6 The 2,5-Dihydrofuran in in the large ($5^{12}6^4$) cage of **a** (2,5-dihydrofuran + H_2O) hydrate, and **b** (2,5-dihydrofuran + methane) hydrate obtained by Rietveld analysis (gray, oxygen in water host molecule; blue, oxygen in guest molecule; red, carbon in guest molecule; hydrogen atoms in water host molecule and guest molecule are omitted)

Conclusions

In summary, we identified the crystal structure of 2,5-dihydrofuran and 2,3-dihydrofuran clathrate hydrate systems with/without methane help gas. The crystal structure of 2,5-dihydrofuran and 2,3-dihydrofuran clathrate hydrate systems with/without methane help gas represents the structure II clathrate hydrate with the cubic *Fd-3m* space group. During the methane inclusion behavior, we observed the decrease of lattice parameters for both 2,5-dihydrofuran and 2,3-dihydrofuran clathrate hydrates. The position of 2,5-dihydrofuran or 2,3-dihydrofuran molecule is almost at the center of large $5^{12}6^4$ cages of (2,5-dihydrofuran + H_2O) or (2,3-dihydrofuran + H_2O) clathrate hydrates, but is off-centered at the center of large $5^{12}6^4$ cages of the binary (2,5-dihydrofuran + CH_4) or (2,3-dihydrofuran + CH_4) clathrate hydrates. And then, there is an increase of guest–host interaction via possible hydrogen bonding interactions during the methane inclusion behaviors. These results provide

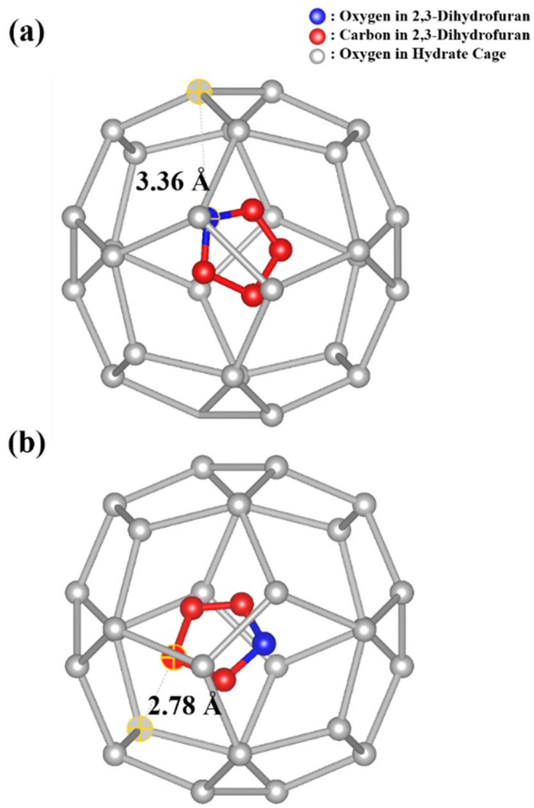

Fig. 7 The 2,3-Dihydrofuran in in the large ($5^{12}6^4$) cage of **a** (2,3-dihydrofuran + H_2O) hydrate, and **b** (2,3-dihydrofuran + methane) hydrate obtained by Rietveld analysis (gray, oxygen in water host molecule; blue, oxygen in guest molecule; red, carbon in guest molecule; hydrogen atoms in water host molecule and guest molecule are omitted)

useful insights into the complex nature of host–guest inclusion chemistry.

Supplementary Information The online version contains supplementary material available at https://doi.org/10.1007/s11814-024-00116-2.

Acknowledgements This study was supported by the National Research Foundation of Korea (NRF) grants (NRF-2021R1F1A1049420) funded by the Korea government (MSIT; Ministry of Science and ICT). This study was also supported by the Korea Institute of Energy Technology Evaluation and Planning (KETEP) and the Ministry of Trade, Industry & Energy (MOTIE) of the Republic of Korea (No. 20224000000080). Nuclear magnetic resonance (NMR) experiments are performed at Bruker AVANCE II + 400 MHz NMR system in KBSI Seoul Western Center. Powder X–Ray diffraction (PXRD) patterns are collected from the beamline (2D) at Pohang Accelerator Laboratory.

References

1. F. Ning, Y. Yu, S. Kjelstrup, T.J.H. Vlugt, K. Glavatskiy, Energy Environ. Sci. **5**, 6779 (2015)
2. G. Bhattacharjee, M.N. Goh, S.E.K. Arumuganainar, Y. Zhang, P. Linga, Energy Environ. Sci. **13**, 4946 (2020)
3. Y. Zhang, J. Zhao, G. Bhattacharjee, H. Xu, M. Yang, R. Kumar, P. Linga, Energy Environ. Sci. **15**, 5362 (2022)
4. W. Wang, C.L. Bray, D.J. Adams, A.I. Cooper, J. Am. Chem. Soc. **130**, 11608 (2008)
5. H.P. Veluswamy, A. Kumar, Y. Seo, J.D. Lee, P. Linga, Appl. Energy. **216**, 262 (2018)
6. E.D. Sloan, Nature. **426**, 353 (2003)
7. E.D. Sloan, C.A. Koh, *Clathrate Hydrates of Natural Gases* (CRC Press, Boca Raton, 2008)
8. K.H. Park, D.H. Kim, M. Cha, Chem. Eng. J. **421**, 127835 (2020)
9. J. Javanmardi, K. Nasrifar, S.H. Najibi, M. Moshfeghian, Appl. Therm. Eng. **25**, 1708 (2005)
10. V.R. Belosludov, Y.Y. Bozhko, K.V. Gets, O.S. Subbotin, Y. Kawazoe, J. Phys. Conf. Ser. **1128**, 012084 (2018)
11. H. Mimachi, S. Takeya, A. Yoneyama, K. Hyodo, T. Takeda, Y. Gotoh, T. Murayama, Chem. Eng. Sci. **118**, 208 (2014)
12. A. Falenty, W.F. Kuhs, M. Glockzin, G. Rehder, Energ. Fuel. **28**, 6275 (2014)
13. W.F. Hao, J.Q. Wang, S.S. Fan, W.B. Hao, Energ. Convers. Manage. **49**, 2546 (2008)
14. M.-K. Kim, G. Han, H. Kim, J. Yu, Y. Lee, T. Song, J. Park, Y.-H. Kim, Y.-H. Ahn, Korean J. Chem. Eng. **40**, 1063 (2023)
15. D.W. Kang, W. Lee, Y.-H. Ahn, J.W. Lee, Chem. Eng. J. **411**, 128512 (2021)
16. Z.G. Sun, R. Wang, R. Ma, K. Guo, S. Fan, Energ. Convers. Manage. **44**, 2733 (2003)
17. H.P. Veluswamy, A. Kumar, R. Kumar, P. Linga, Appl. Energy. **188**, 190 (2017)
18. J. Lee, Y.K. Jin, Y. Seo, Chem. Eng. J. **338**, 572 (2018)
19. S. Baek, W. Lee, J. Min, Y.-H. Ahn, D.W. Kang, J.W. Lee, Korean J. Chem. Eng. **37**, 341 (2020)
20. Z.G. Sun, S.S. Fan, K.H. Guo, L. Shi, Y.K. Guo, R.Z. Wang, J. Chem. Eng. Data. **47**, 313 (2002)
21. B. Tohidi, A. Danesh, A.C. Todd, R.W. Burgass, K.K. Ostergaard, Fluid Ph. Equilib. **138**, 241 (1997)
22. Y.J. Lee, T. Kawamura, Y. Yamamoto, J.H. Yoon, J. Chem. Eng. Data. **57**, 3543 (2012)
23. H. Komatsu, H. Yoshioka, M. Ota, Y. Sato, M. Watanabe, R.L. Smith, C.J. Peters, J. Chem. Eng. Data. **55**, 2214 (2010)
24. Y, -T. Seo, H. Lee, Korean J. Chem. Eng. **20**, 1085 (2003)
25. Q. Lv, X. Li, Energy Proc. **142**, 3264 (2017)
26. I. Majerz, J. Comput. Aided Mol. Des. **32**, 1247 (2018)
27. R.E. Hawkins, D.W. Davidson, J. Phys. Chem. **70**, 1889 (1966)
28. M. Mozafari, J.-C. Brodovitch, L. Chandrasena, P.W. Percival, J. Phys. Chem. A **120**, 8521 (2016)
29. J.W. Shin, K. Eom, D. Moon, J. Synchrotron Radiat. **23**, 369 (2016)
30. K.H. Park, D.H. Kim, M. Cha, Chem. Phys. Lett. **779**, 138869 (2021)
31. K.H. Park, D.H. Kim, M. Cha, J. Phys. Chem. C **126**, 13585 (2022)
32. K.H. Park, D.H. Kim, M. Cha, Chem. Phys. Lett. **806**, 140054 (2022)
33. D.H. Kim, K.H. Park, M. Cha, J.-H. Yoon, Korean J. Chem. Eng. **39**, 2211 (2022)
34. R.A. Young, *The Rietveld Method*, OXFORD (2002)
35. S. Takeya, K.A. Udachin, I.L. Moudrakovski, R. Susilo, J.A. Ripmeester, J. Am. Chem. Soc. **132**, 524 (2010)
36. J. Rodriguez-Carvajal, Phys. B **192**, 55–69 (1993)
37. V. Favre-Nicolin, R. Černý, J. Appl. Crystallogr. **35**, 734 (2002)
38. BIOVIA, Dassault Systèmes, San Diego (2022)

39. T. Kawamura, S. Takeya, M. Ohtake, Y. Yamamoto, Chem. Eng. Sci. **66**, 2417 (2011)
40. K. Momma, F. Izumi, J. Appl. Crystallogr. **44**, 1272 (2011)

Publisher's Note Springer Nature remains neutral with regard to jurisdictional claims in published maps and institutional affiliations.